Feedback Control for Active Noise Reduction in Headsets

J. Graf[1], E. Reithmeier[2]

[1] Leibniz Universität Hannover, Germany, Email: jens.graf@imr.uni-hannover.de

[2] Leibniz Universität Hannover, Germany, Email: eduard.reithmeier@imr.uni-hannover.de

Introduction

With regard to production costs, control strategies for commercial ANR-headsets (Active Noise Reduction) have to be realized simple and efficient. Therefore, the implementation of computationally expensive algorithms, which require fast and expensive digital signal processors, is not favorable. Besides an expensive DSP, further costs are caused by a reference microphone that is required in case of feedforward control. In contrast to the feedforward control approach, the feedback control strategy does not use such a reference microphone [1-3] and thus, the reference microphone as well as the associated analog input circuit can be saved.

In this paper a time discrete feedback control approach is suggested that consists of two controller parts. One part is formed by a non-adaptive standard feedback control loop and the second part consists of an adaptive IMC (internal model control) controller [3]. The non-adaptive controller guarantees steady-state noise reduction and the overall performance of the ANR-system is improved by the adaptive IMC controller. Additionally, a neutralization filter is introduced that accomplishes a flatting of the secondary path. In comparison to the implementation without neutralization filter significant computational effort can be saved while retaining the ANR-performance.

Non-Adaptive Feedback Control

One major advantage of the non-adaptive feedback control approach is its simple realizability as a non-adaptive IIR-filter. Additionally, non-adaptive control strategies provide steady-state noise reduction since no adaptation has to be accomplished. These advantages are the reason for using the non-adaptive standard feedback control loop to provide the basic noise reduction for the subsequently described combined control approach.

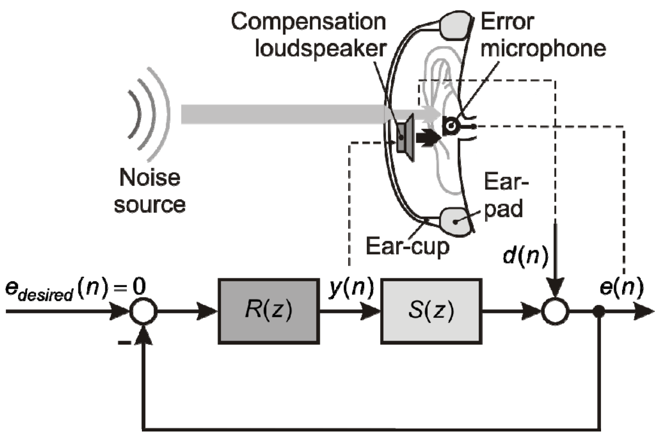

Figure 1: Non-adaptive standard control loop. Upper part: Schematic drawing of the ear-cup. Lower part: block diagram with controller $R(z)$ and secondary path $S(z)$.

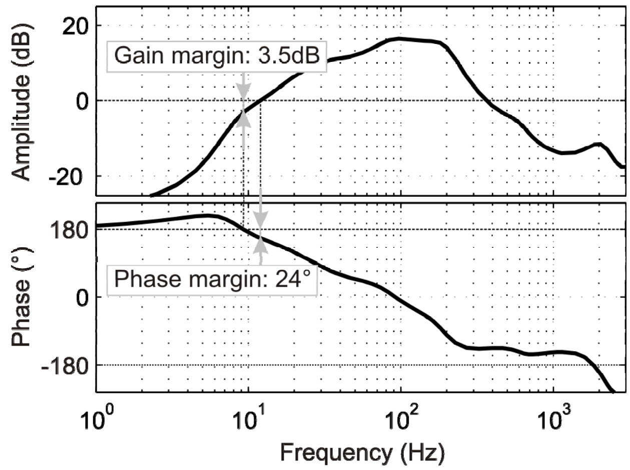

Figure 2: Open loop bode-plot.

In the upper part of Figure 1, a schematic drawing of the used circum aural headset can be seen. The compensation loudspeaker that outputs the out-of-phase antinoise as well as the error microphone is located inside the ear-cup. The error microphone reads the error signal $e(n)$ and feeds it back to the controller $R(z)$. The output of this controller $y(n)$, is fed to the compensation loudspeaker and thus the antinoise and the disturbing noise $d(n)$ destructively interfere. Hereby, the transfer behavior from the compensation loudspeaker to the error microphone is represented by the so called secondary path $S(z)$.

The design of the feedback controller $R(z)$ can be seen as a dual problem: On one hand, effective noise reduction is favorable but on the other hand, the stable closed feedback loop has to be guaranteed [1-5]. As depicted in Figure 2, the stability of the closed loop is confirmed. It can be seen that according to the simplified nyquist criterion, the designed controller $R(z)$ results in a phase margin of approximately 24 degrees and a gain margin of 3.5 dB. In this conjunction, it has to be mentioned that these margins are only valid in case of a non-variant secondary path $S(z)$. In case of a real world application, the secondary path $S(z)$ underlies small variations depending on the anatomy of the person bearing the headset. However, in the framework of many experiments with different test persons, the stability of the designed controller was validated.

Combined Feedback Control

Even though the non-adaptive feedback control approach has many advantages regarding robustness and simplicity, optimal control is not feasible. This results from the fact that the design of $R(z)$ is always a trade off between stability and noise reduction bandwidth as well as active noise reduction performance. A further problem of the non-adaptive

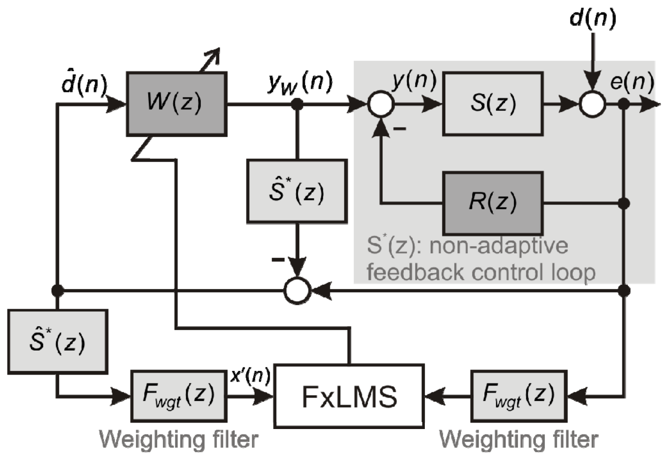

Figure 3: Non-adaptive standard control loop linked to the adaptive IMC controller *W*(*z*).

controller is that an adaptation to the spectrum of the disturbing noise is not feasible. These mentioned issues lead to a limited noise reduction performance and a fixed noise reduction bandwidth.

In order to improve the noise reduction performance, the non-adaptive controller is combined with an adaptive IMC controller as depicted in Figure 3. The IMC control principle uses an estimated signal $\hat{d}(n)$ of the disturbing noise $d(n)$ as the input of the adaptive controller $W(z)$.

The shown combined control results in a secondary path that involves the non-adaptive closed feedback loop [3], [4]:

$$S^*(z) = \frac{S(z)}{1+R(z)S(z)}. \qquad (1)$$

According to the IMC principle, a model of this secondary path is used to compute the estimated disturbance $\hat{d}(n)$ as well as to generate the filter reference signal in the reference path.

Considering the transfer function of the secondary path $S^*(z)$ as well as its model $\hat{S}^*(z)$, the disturbance transfer function of the combined control results:

$$\frac{E(z)}{D(z)} = \frac{1}{1+R(z)S(z)} \cdot \frac{1+W(z)\hat{S}^*(z)}{1+W(z)(\hat{S}^*(z)-S^*(z))}. \qquad (2)$$

The control objective of the combined ANR-controller is the minimization of the residual error $E(z)$. In order to minimize the error signal, on one hand, the feedback controller $R(z)$ has to maximize the denominator of the first term of equation (2). On the other hand, the error signal is reduced in case the IMC adaptive controller $W(z)$ approximates the optimal IMC controller transfer function that is given by the negative inverse the secondary path model:

$$W(z) = -\frac{1}{\hat{S}^*(z)}. \qquad (3)$$

It has to be remarked that the optimal controller according to this equation is not feasible to realize. One reason for this is the fact that $\hat{S}^*(z)$ usually involves time delay. Thus, the required inversion according equation (2) results in a non-causal controller transfer function. Hence, it is only feasible to realize the causal part which is the minimum phase part of equation (3).

Another problem in conjunction with the IMC control approach is the variability of $S^*(z)$ during operation. Such variations occur, e.g. in case of different ear anatomies or if the ear-cup leakage changes. However, these variations can be accounted for using an adaptation algorithm that permanently adapts the parameters of the controller $W(z)$. A further problem regarding variations of the secondary path has to be considered when investigating the stability of the disturbing transfer function (2). In case of modeling errors of the secondary path model, the denominator of equation (2) is affected by the adaptive parameters. However, in case of modeling inaccuracies that are of multiplicative type, the stability of equation (2) can be guaranteed [5].

For the implementation of $W(z)$ an FIR-filter structure is chosen. The advantage of FIR-filters is the inherent stability and thus the adaptation process never results in an instable controller transfer function $W(z)$. For the adaptation of the parameters of $W(z)$, the MSE (mean square error) cost function is usually chosen:

$$J = E\left[e^2(n)\right]. \qquad (4)$$

This cost function, in conjunction with an FIR-filter $W(z)$, results in a convex performance surface. Thus, the adaptation of the parameters is achieved using the well known Filtered-x-Least-Mean-Square adaptation algorithm [1], [2]:

$$\mathbf{w}(n+1) = \mathbf{w}(n) + \mu \cdot \mathbf{x}'(n)e(n). \qquad (5)$$

In this parameter update equation, the small constant μ refers to the step-size which determines the adaptation velocity of the algorithm and the vector $\mathbf{x}'(n)$ contains the time series of the filtered reference signal $x'(n)$:

$$\mathbf{x}'(n) = \left[x'(n) \quad x'(n-1) \quad \dots \quad x'(n-L+1)\right]^T. \qquad (6)$$

The length L of $\mathbf{x}'(n)$ has to be of same size as the parameter vector $\mathbf{w}(n)$. In block diagrams of this paper, the so obtained adaptation algorithm is represented using a transmission block labeled “FxLMS”.

According to Figure 3, the filtered reference signal $x'(n)$ is generated by filtering the reference $x(n)$ with the secondary path model $\hat{S}^*(z)$ and a subsequent filtering with the so called frequency selective filter or weighting filter $F_{wgt}(z)$. This frequency selective filter shapes the error signal which leads to the cost function:

$$J = E[(e(n) * \underbrace{f_{wgt}(n)}_{\text{Impulse response of } F_{wgt}(z)})^2]. \qquad (7)$$

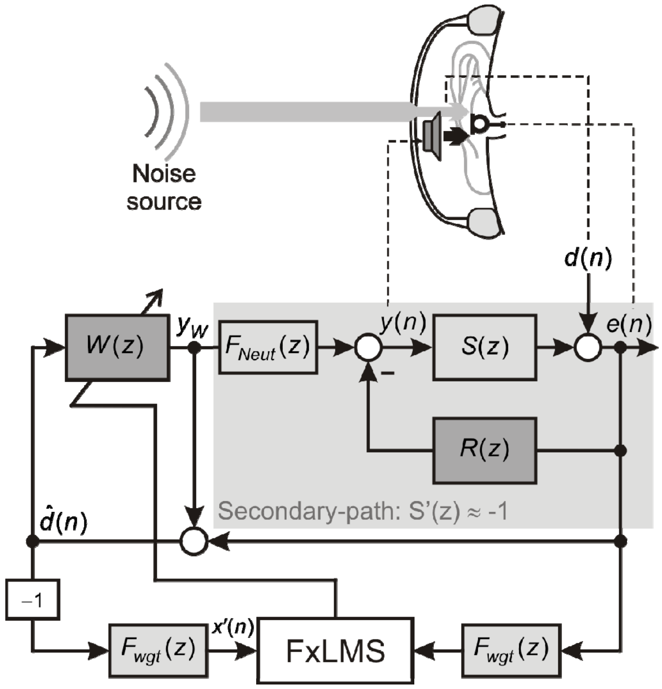

Figure 4: Non-adaptive standard control loop linked to the adaptive IMC controller $W(z)$. Using the neutralization filter results in a simplified model $S'(z)\approx-1$.

This cost function is the basis for the minimization problem of the adaptive algorithm. Therefore, the frequency selective filter permits the adaptation to an intended frequency range that is selected by the design of $F_{wgt}(z)$. Since the IMC feedback control approach does not permit the reduction of very low as well as higher frequencies components, the frequency selective filter is designed as a band-pass filter with cut-off frequencies of about 100 Hz and 1000 Hz.

Secondary-Path Neutralization

The implementation of the above described linked controller consisting of the adaptive IMC-control with a subordinated standard feedback control loop. The implementation according to Figure 3 results in effective noise reduction using approximately 80 adaptive parameters. In this paragraph a neutralization filter is introduced that permits the decrease of the number of adaptive parameters. As shown in Figure 4, the neutralization filter is connected ahead of $\hat{S}^*(z)$ and again a modified secondary-path results:

$$S'(z) = S^*(z)\cdot F_{neut}(z). \tag{8}$$

The objective is to shape the frequency response of $S'(z)$ in the desired frequency range so that:

$$\left|S'(z)\right| \approx 1 \quad \text{and} \quad \arg\left(S'(z)\right) \approx -180°. \tag{9}$$

In fact, due to time delay, this neutralization is only valid for low frequencies. Thus, in this frequency range, the exact model of $S'(z)$ can be replaced using the simplification:

$$\hat{S}'(z) = -1. \tag{10}$$

This simplification according to equation (10) is illustrated in Figure 5. Using this simplification, the two required filter

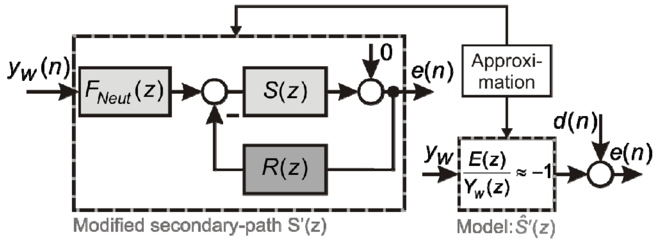

Figure 5: The modified secondary-path $S'(z)$ is adequately approximated using the model $S'(z)\approx-1$.

operations with the model $\hat{S}'(z)$ can be replaced by a simple multiplication with the constant factor of -1.

The resulting control structure including the neutralization $F_{neut}(z)$ filter as well as the simplified model (10) is shown in Figure 4. According to the illustrated block diagram, the control law of the combined ANR-controller is obtained:

$$y(n) = Z^{-1}\left\{F_{neut}(z)W(z)\hat{D}(z) - R(z)E(z)\right\}. \tag{11}$$

The suggested combined feedback ANR-control strategy with neutralized secondary path is implemented in a DSP-platform. As the acoustic front-end, the commercial product HMEC350 is used and all required electrical connections of the error microphones as well as the compensation loudspeakers are lead out and linked to the DSP-processor.

Noise Reduction Performance

In order to verify the ANR-performance of the proposed control approach, the headset is exposed to noise that is recorded inside the cockpit of a helicopter. As can be seen in Figure 6, the spectrum of this noise consists of broadband noise with most of the signal power in the lower frequency range.

The active noise reduction performance of the ANR-controller is measured while the headset is located on a test-head. The test-head is equipped with an ear-simulator that includes an internal ear-microphone. This microphone is used for the noise reduction measurements. In order to verify the proposed combined controller with secondary path neutralization, two experiments are conducted.

In case of the first experiment, only 10 adaptive parameters

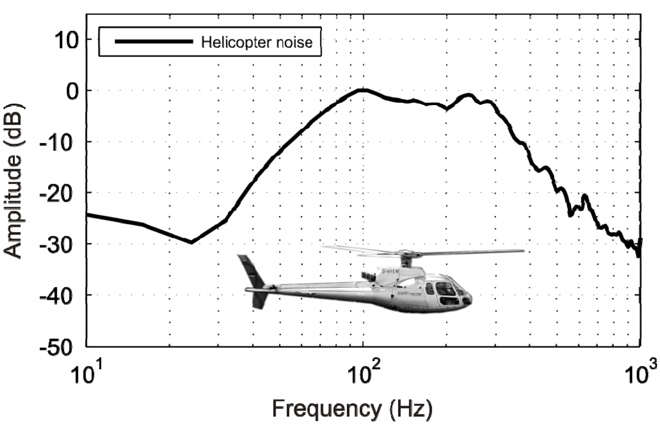

Figure 6: Helicopter cockpit noise.

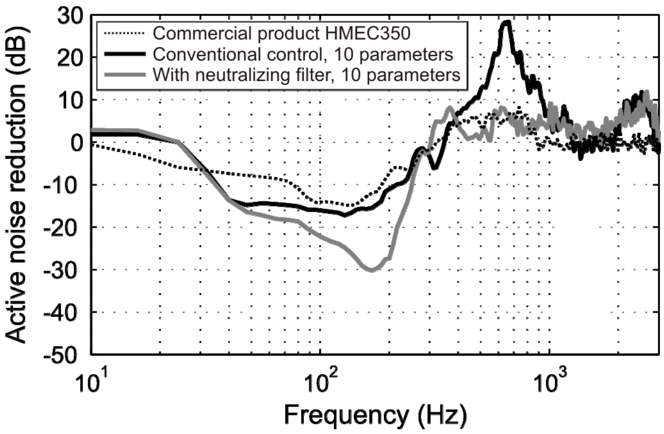

Figure 7: Active noise reduction performance. Only 10 adaptive parameters are used.

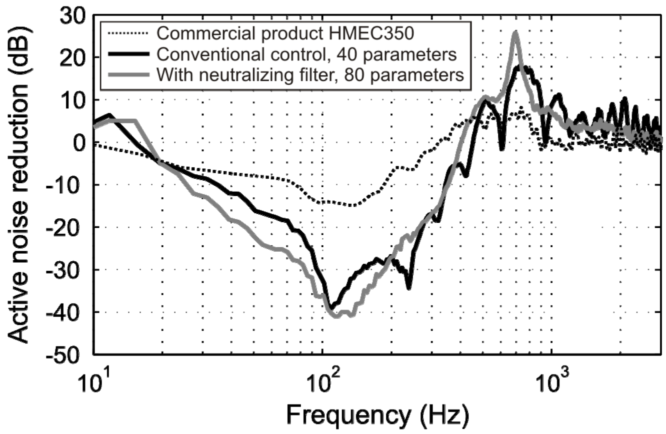

Figure 8: Active noise reduction performance using an increased number of adaptive parameters.

are used for both the conventional implementation as well as the implementation with secondary path neutralization. The noise reduction result of this experiment is shown in Figure 7. It can be seen that the commercial product HMEC350 (dashed line) and the conventional implementation according to Figure 3 (black solid line) are outperformed by the combined controller with neutralization filter (grey solid line). In the low frequency range, the noise reduction performance is improved up to 15 dB and in the higher frequency range the amplification of the disturbing noise is avoided.

In the framework of the second experiment, 80 adaptive parameters are used for the conventional implementation. This number of parameters leads to a noise reduction performance that cannot be significantly improved solely by further increasing the number of adaptive parameters. It turned out that in case of the combined controller with neutralization filter, only 40 adaptive parameters were necessary to achieve a noise reduction performance similar to the performance of the conventional implementation with 80 adaptive parameters. The noise reduction performance of this experiment is shown in Figure 8. Both combined adaptive controllers outperform the commercial product up to approximately 20 dB in the frequency range from 20 Hz to 450 Hz. For the frequency range above 450 Hz, the noise is amplified by the adaptive controllers. However, this is not a problem since these higher frequencies feature only small amplitudes within the spectrum of the disturbing noise.

Both presented experiments show that the control approach with neutralization of the secondary path permits the saving of adaptive parameters and therefore results in an ANR-controller with limited computational effort.

Conclusion

In the framework of this paper, the non-adaptive standard feedback control loop is linked to an adaptive IMC (internal model control) controller. In contrast to the conventional implementation of such a combined control approach, additionally, the secondary path is neutralized using a neutralizing filter. The noise reduction performance of the combined controller with neutralizing filter is compared to a conventional implementation without this filter as well as a commercial aviation headset. The noise reduction measurements show that the ANR-performance of the proposed control strategy outperforms the commercial product. In comparison to the conventional combined control, a large number of adaptive parameters can be saved.

References

[1] S.J. Elliott, Signal Processing for Active Control, Academic Press, San Diego, 2001

[2] S.M. Kuo and D.R. Morgan, Active Noise Control Systems Algorithms and DSP Implementations, Wiley-Interscience Publication, New York, 1996

[3] Y. Song, Y. Gong and S.M. Kuo, A Robust Hybrid Feedback Active Noise Cancellation Headset, IEEE Transactions on Speech and Audio Processing, Vol. 13(4), pp. 607-17, 2005

[4] E. Reithmeier and J. Graf, Combination of non-Adaptive and Adaptive Control Strategies for Active Noise Reduction in Headsets, 9th International Conference on Motion and Vibration Control, Movic, Munich, 2008

[5] G. Feng and R. Lozano, Adaptive Control Systems, Newnes, Oxford, 1999